Tracing the photodissociation probability of H_2^+ in intense fields using chirped laser pulses

Vaibhav S. Prabhudesai,[1,*] Uri Lev,[2,†] Adi Natan,[1,‡] Barry D. Bruner,[1] Adi Diner,[1] Oded Heber,[2] Daniel Strasser,[2,3] D. Schwalm,[2,4] Itzik Ben-Itzhak,[5] J. J. Hua,[5] B. D. Esry,[5] Yaron Silberberg,[1] and Daniel Zajfman[2]

[1]*Department of Physics of Complex Systems, Weizmann Institute of Science, IL-76100 Rehovot, Israel*

[2]*Department of Particle Physics, Weizmann Institute of Science, IL-76100 Rehovot, Israel*

[3]*Institute of Chemistry, Hebrew University, IL-91904 Jerusalem, Israel*

[4]*Max-Planck-Institut für Kernphysik, D-69117 Heidelberg, Germany*

[5]*J. R. Macdonald Laboratory, Kansas State University, Manhattan, Kansas 66506, USA*

(Received 30 September 2009; published 3 February 2010)

The temporal evolution of the dissociation probabilities for various vibrational levels of H_2^+ is observed in terms of shifts in the kinetic energy release dissociation spectra, induced by linearly chirped intense laser pulses. In contrast to previous observations, in which no dependence on the chirp sign was observed, the energy spectrum reported here shows peak shifts, up for negative chirp and down for positive chirp. For some vibrational levels, dissociation takes place early on in the pulse; hence, care must be taken while interpreting the effect of pulse duration in photodissociation studies. This interpretation is supported by numerical solutions of the time-dependent Schrödinger equation.

DOI: 10.1103/PhysRevA.81.023401 PACS number(s): 33.80.Gj

I. INTRODUCTION

The fields of ultrafast strong-field–matter interaction in general and photodissociation and ionization processes in particular have attracted considerable attention in recent years with the advent of ultrashort intense laser sources and momentum imaging techniques [1–14]. In these investigations, the simplest molecules, molecular hydrogen and ionic H_2^+, have served as model systems to explore the complex dynamics arising from the presence of strong light fields. Many interesting phenomena such as bond softening and above-threshold dissociation have been experimentally demonstrated in these molecular systems [4,10,11,14–16]. Thus far, laser peak intensity, carrier envelope phase [7], and pulse duration have mainly been used to study these phenomena.

Apart from the peak intensity and duration, femtosecond pulses are also characterized by their broad spectral content. One can manipulate the intrinsic time and frequency correlation within the laser pulse and, hence, its temporal shape by controlling the spectral phase [17]. Linear chirp is the simplest example of such a manipulation; the instantaneous central frequency is swept linearly across the bandwidth of the pulse. Pulses in which the lower frequencies come ahead are referred to as positively chirped. In previous studies of intense field photodissociation of H_2^+, linear chirp has been used to manipulate the temporal width and the peak power of the laser pulses. For example, Frasinski *et al.* [6] demonstrated the manipulation of bond hardening using linearly chirped pulses. But none of these studies reported any significant effect caused by the linear chirp *sign* on the H_2^+ photodissociation.

For H_2^+, the typical dissociation time on the first repulsive excited state is of the order of 10 fs. In principle, for such fast dynamics, linear chirp can be used to map the instant of dissociation from different vibrational levels within a much longer (100-fs) laser pulse. Here we report the results of experiments performed with linearly chirped intense broadband laser pulses and an H_2^+ ion beam as the target. The results clearly show distinct shifts in the kinetic energy release (KER) spectra, which we attribute to the time of dissociation within the pulse. The chirp sign is used to verify this correlation. This understanding is supported by our numerical solution of the time-dependent Schrödinger equation (TDSE).

II. EXPERIMENTAL

In our experiments, a well-collimated pulsed 4-keV H_2^+ ion beam (0.5 mm diameter, 3 μs duration, 1 kHz repetition rate) with a Franck-Condon distribution of vibrational states is produced in a Nielsen ion source [18]. It is directed through a longitudinal electrostatic spectrometer similar to the one used in Refs. [8,15] into a 3-mm Faraday cup located in front of a position-sensitive microchannel plate (MCP) detector as shown in Fig. 1. The timing information of the fragments reaching the detector is derived from the MCP signal, while the position information is obtained from a phosphor screen located at the back of the MCP, using a CCD camera along with a home-built frame grabber [19]. The timing and position signals collected for both fragments in coincidence are used to reconstruct the complete three-dimensional momentum information of the fragmentation process on an event-by-event basis.

A Ti:sapphire multipass amplifier (Femtolasers GmbH) is used to produce intense ultrashort laser pulses (795 nm, 30 fs full width at half maximum [FWHM], at 1 kHz). The pulses are steered into a conventional 4f pulse shaper [17] that consists of 1000 lines/mm gratings, 20-cm cylindrical mirrors, and a programmable liquid crystal spatial light modulator (SLM; Jena Phase SLM-640) placed in the Fourier plane. The SLM is used as a dynamic filter for the spectral phase of the pulses [20]. With the help of the pulse shaper we can precisely control the chirp rate and sign while compensating for any higher order dispersion. Furthermore, the spectral content of the pulse can be easily manipulated using an amplitude mask in the Fourier plane. As illustrated in Fig. 1, the pulses were linearly polarized in the $\hat{y}$ direction, perpendicular to the direction of the ion

*Vaibhav.Prabhudesai@weizmann.ac.il
†Uri.Lev@weizmann.ac.il
‡Adi.Natan@weizmann.ac.il

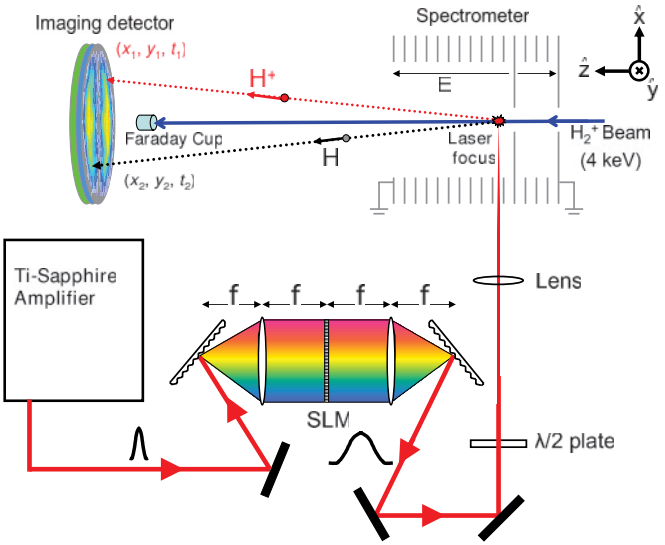

FIG. 1. (Color online) A schematic of the experimental setup.

beam propagating along $\hat{z}$. The propagation direction of the laser beam was along the $\hat{x}$ direction and it was focused onto the ion beam by a lens with focal length $f = 30$, producing an 80-μm focal waist with peak intensity of up to $I_0 = 2 \times 10^{13}$ W/cm^2.

III. RESULTS

Figures 2(a) and 2(b) show a density plot of the distribution of dissociation signal as a function of $\cos\theta$ and KER, where θ is the angle of the fragmentation axis with respect to the laser polarization direction in the molecular center-of-mass frame for a negatively and positively chirped laser pulse, respectively. The chirped pulse was created by stretching the 30-fs transform-limited pulse to 120 fs by applying a quadratic phase that corresponds to a group delay dispersion (GDD) of 650 fs^2. The bandwidth of the pulses was about 40 nm FWHM. The events observed in these plots are mainly due to the photodissociation of the $v \geqslant 7$ vibrational levels of H_2^+. It can be easily seen that, in both spectra, the KER peak positions do not coincide with the expected field-free values ($E_{\mathrm{ker},v}$, indicated by vertical dashed lines) given by $E_{\mathrm{ker},v} = h\nu - (D_0 - E_v)$, where $h\nu$ is photon energy, D_0 is the final energy at the dissociation limit, and E_v is the initial eigenvalue of vibrational state v. Moreover, the KER peaks of the different vibrational levels shift to higher energy for negative chirp and to lower energy for positive chirp. As discussed later, this opposite dependence on the chirp sign is a consequence of the dissociation taking place well before the peak of the laser pulse. Furthermore, this result suggests that caution should be taken when exploring pulse duration effects by chirping the pulse because the results may depend on the chirp sign used.

A 120-fs pulse can also be produced by reducing the laser bandwidth, without introducing chirp. We generated such pulses by placing an amplitude mask in the Fourier plane of the pulse shaper assembly, which sets a full bandwidth of 18 nm around the central wavelength. The distribution in $\cos\theta$ and KER produced by such a pulse with a peak intensity of $I_0 = 5 \times 10^{12}$ W/cm^2 is shown in Fig. 2(c), while the

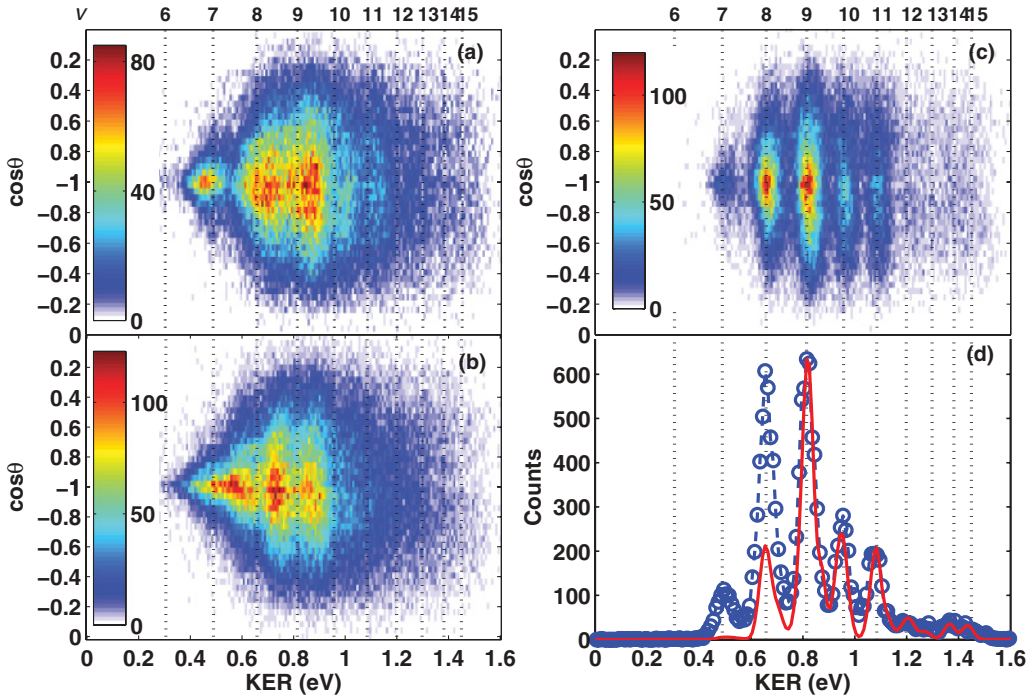

FIG. 2. (Color online) Charts showing $\cos\theta$ vs kinetic energy release (KER) spectra of H_2^+ photodissociation by (a) negatively chirped pulse; (b) positively chirped pulse, both with peak intensity ($I_0 = 2 \times 10^{13}$ W/cm^2); and (c) zero chirp pulse ($I_0 = 5 \times 10^{12}$ W/cm^2 with about half the bandwidth). All pulse envelopes have the same duration of 120 fs. (d) Projection of the data shown in panel (c) onto the KER axis for $|\cos\theta| \geqslant 0.9$. The solid line is the KER spectrum, calculated as described in the main text. The dotted vertical lines indicate the expected position of the vibrational-level peaks for 795-nm photons.

corresponding projection onto the KER axis for $|\cos\theta| \geqslant 0.9$ is displayed in Fig. 2(d). Here the vibrational-level peaks are well separated and the overall width of each peak is due to the convolution of the systematic experimental resolution (estimated to be about 40 meV around 1 eV), the energy spread due to approximately 18 nm (35 meV) bandwidth of the laser pulse, and the finite rotational temperature of the ion beam [21]. The KER peak positions in Fig. 2(d) match nicely with the expected field-free values. The solid line shows the KER spectrum computed using first-order perturbation theory [22] and incorporating the experimental effects of finite target density, the intensity averaging over the interaction volume, the resolution of the imaging setup, and the finite rotational temperature. The vibrational distribution of the H_2^+ target is assumed to be the Franck-Condon distribution, and the rotational distribution of the target ions is derived from the initial temperature of the neutral H_2 gas in the ion source [21]. The ion-source temperature is used as a free parameter and the best value is found to be 800° C, which is in accordance with the expected value for the ion source used. The computed spectrum is normalized to the data at the $v = 9$ peak and it fits the experimental data very well for vibrational levels above $v = 9$. In contrast, the calculation underestimates the lower vibrational levels, indicating the onset of intense field effects, where the perturbation theory fails. This finding is also evident from the narrower angular distribution obtained in this KER region [Fig. 2(c)]. Noting that the laser peak intensity in this measurement is comparable to that of our chirped pulses, it can also be concluded that ac stark shifts associated with the vibrational levels $v \geqslant 8$ are too small to account for the KER peak shifts observed for the chirped pulses [Figs. 2(a) and 2(b)].

To get further insight into the cause of these KER shifts, we computed the time evolution of the dissociation probabilities by solving the TDSE numerically using the method described in Ref. [15] for the 30-fs bandwidth limited laser pulse centered at 785 nm with appropriate chirp. The internuclear axis was kept fixed along the laser polarization, allowing nuclear vibration on the coupled $1s\sigma_g$ and $2p\sigma_u$ channels. The time envelope of the pulse, which is independent of the chirp sign, is shown in Fig. 3(a). The resulting time-dependent dissociation probabilities for both positive and negative chirp for the relevant initial vibrational states are shown in Figs. 3(b)–3(e) for a peak intensity of 5×10^{12} W/cm^2. Figure 3(f) shows the calculated KER spectrum, taking into account intensity averaging over the focal volume as well as the initial vibrational population of the H_2^+ target. These calculations do not include the initial rotational distribution.

For vibrational levels from $v = 8$ and above, the calculated dissociation probabilities become saturated about 50–100 fs before the pulse reaches its peak intensity. Since the temporal order of the frequency within the laser pulse depends on the sign of the chirp, it leads to shifts in the KER peaks, as demonstrated by the calculated KER spectrum shown in Fig. 3(f). Hence, the shift of the KER peak for a given vibrational level is the manifestation of the most probable time of dissociation for each vibrational level within the laser pulse. For example, for positively chirped pulses (lower to higher spectral frequency sweep), dissociation early in the

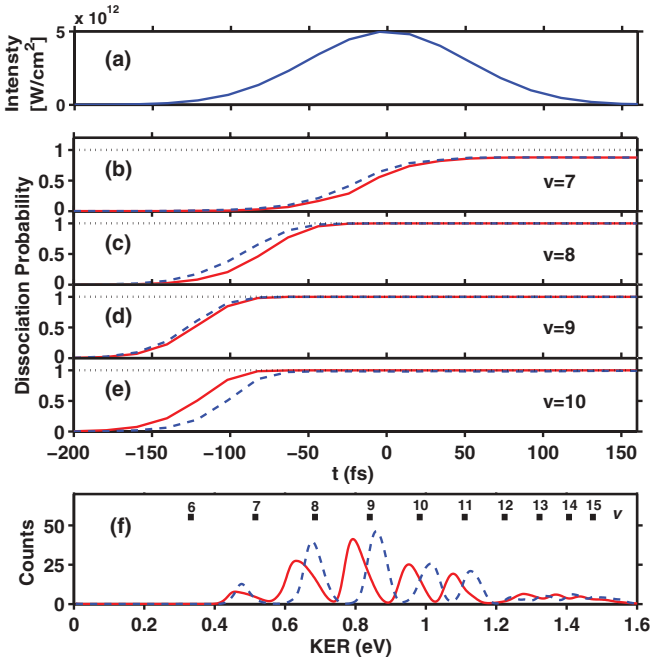

FIG. 3. (Color online) (a) Time-dependent laser intensity envelope and (b)–(e) calculated dissociation probability for a few vibrational states of H_2^+ as a function of time, for negative (dashed) and positive (solid) chirp pulse with a peak intensity of 5×10^{12} W/cm^2. Note that the dissociation for vibrational levels $v \geqslant 8$ becomes saturated about 50–100 fs before the pulse peaks. (f) Calculated KER spectra incorporating intensity averaging over the focal volume and the initial vibrational (but not rotational) distribution of the molecular target.

pulse means that it takes place at lower frequencies compared to the central frequency of the pulse, leading to dissociation events with lower KER. From the evolution of the dissociation probability, it can be expected that the KER peak shift will be a maximum for vibrational level $v = 9$ and a minimum for lower vibrational states. Moreover, the shifts in the KER peaks will grow with increasing intensity as the dissociation occurs at an even earlier time.

We demonstrated these intensity-dependent shifts by carrying out systematic measurements of the KER spectra for 120 fs chirped pulses with increasing peak intensities ranging over two orders of magnitude from $I_0 = 1 \times 10^{11}$ to $I_0 = 2 \times 10^{13}$ W/cm^2. The resulting KER spectra are presented in Figs. 4(a) and 4(b) for negatively and positively chirped pulses, respectively. The plots are normalized to the estimated total number of target ions and corrected for the detector dead time.

For the lowest intensity pulses ($I_0 = 1 \times 10^{11}$ W/cm^2), the KER peak positions coincide with the predicted field-free "vibrational comb" for both chirp signs, as can be seen from the inset of Fig. 4(a). As the intensity increases, the peaks are found to shift monotonically farther from the field-free value and in opposite directions for the two chirp signs. In the case of positive chirp, they shift to lower KER values, whereas they shift to higher values for negative chirp. At the highest laser intensity investigated, the observed peak

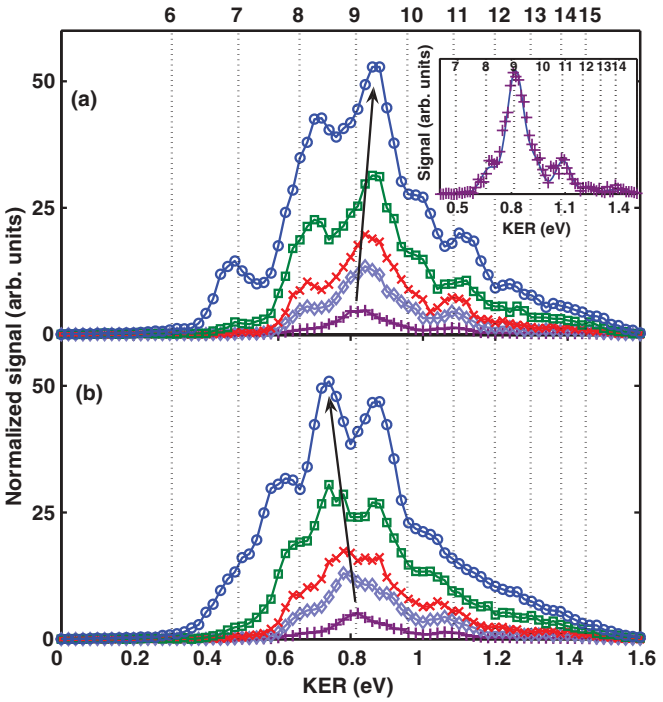

FIG. 4. (Color online) (a) Kinetic energy release (KER) spectra of H_2^+ for negatively and (b) positively chirped pulses taken at different peak intensities: (◯) 2×10^{13}, (□) 7×10^{12}, (×) 2×10^{12}, (◇) 1×10^{12}, and (+) 1×10^{11} W/cm^2. The spectra are generated by summing the signal over all angles. The solid arrows indicate the directional shift in the KER peak position connected with the vibrational level $v = 9$. The inset in panel (a) shows the KER spectrum for the lowest peak intensity along with the calculated spectrum (solid line) using perturbation theory (see text).

shifts between positively and negatively chirped pulses are as large as the vibrational spacings for this molecule. Also, these shifts are found to be different for different vibrational levels, being maximal for $v = 9$. In the case of $v = 9$, the shift in the KER peak is found to be about 50 meV upward and 70 meV downward, for negatively and positively chirped laser pulses with $I_0 = 7 \times 10^{12}$ W/cm^2, respectively. Using these values and the GDD, the time of saturation of the dissociation probability is estimated to be about 100–150 fs before the pulse reaches its highest intensity. The calculated time value from Fig. 3(d) is in good agreement with this estimate. As shown in Fig. 3(b), the dissociation probability for $v = 7$ does not become saturated for the pulses used in the experiment. Hence, this vibrational level encounters the strongest part of the laser pulse. A small shift observed for $v = 7$, as seen in Fig. 4(a), can be possibly attributed to the ac stark shift.

IV. CONCLUSION

To conclude, we have traced the photodissociation probability of vibrational states of H_2^+ in intense photon fields using chirped laser pulses. We demonstrated that the dissociation of individual vibrational states can become saturated at times much before the peak intensity of the laser pulse is reached, which leads, depending on the sign of the chirp, to shifts of the corresponding peaks in the KER spectra in opposite directions. Our result also implies that care has to be taken when interpreting pulse-duration effects in photodissociation studies using chirped pulses.

ACKNOWLEDGMENTS

This work was supported by the Israeli Science Foundation and the Chemical Sciences, Geosciences, and Biosciences Division, Office of Basic Energy Sciences, Office of Science, US Department of Energy.

[1] J. McKenna, A. M. Sayler, B. Gaire, N. G. Johnson, E. Parke, K. D. Carnes, B. D. Esry, and I. Ben-Itzhak, Phys. Rev. A **77**, 063422 (2008).
[2] A. M. Sayler, P. Q. Wang, K. D. Carnes, B. D. Esry, and I. Ben-Itzhak, Phys. Rev. A **75**, 063420 (2007).
[3] H. G. Breunig, A. Lauer, and K.-M. Weitzel, J. Phys. Chem. A **110**, 6395 (2006).
[4] K. Sändig, H. Figger, and T. W. Hänsch, Phys. Rev. Lett. **85**, 4876 (2000).
[5] I. D. Williams *et al.*, J. Phys. B **33**, 2743 (2000).
[6] L. J. Frasinski, J. H. Posthumus, J. Plumridge, K. Codling, P. F. Taday, and A. J. Langley, Phys. Rev. Lett. **83**, 3625 (1999).
[7] M. F. Kling *et al.*, Science **312**, 246 (2006).
[8] I. Ben-Itzhak, P. Q. Wang, J. F. Xia, A. M. Sayler, M. A. Smith, K. D. Carnes, and B. D. Esry, Phys. Rev. Lett. **95**, 073002 (2005).
[9] A. Assion, T. Baumert, U. Weichmann, and G. Gerber, Phys. Rev. Lett. **86**, 5695 (2001).
[10] J. McKenna *et al.*, J. Phys. B **40**, 2607 (2007).
[11] J. H. Posthumus *et al.*, J. Phys. B **33**, L563 (2000).
[12] D. Pavicic, T. W. Hänsch, and H. Figger, Phys. Rev. A **72**, 053413 (2005).
[13] B. Feuerstein, T. Ergler, A. Rudenko, K. Zrost, C. D. Schroter, R. Moshammer, J. Ullrich, T. Niederhausen, and U. Thumm, Phys. Rev. Lett. **99**, 153002 (2007).
[14] J. H. Posthumus, Rep. Prog. Phys. **67**, 623 (2004).
[15] P. Q. Wang, A. M. Sayler, K. D. Carnes, J. F. Xia, M. A. Smith, B. D. Esry, and I. Ben-Itzhak, Phys. Rev. A **74**, 043411 (2006).
[16] J. McKenna *et al.*, Phys. Rev. Lett. **100**, 133001 (2008).
[17] A. M. Weiner, Rev. Sci. Instrum. **71**, 1929 (2000).
[18] K. O. Nielsen, Nucl. Instrum. **1**, 289 (1957).
[19] D. Strasser, K. G. Bhushan, H. B. Pedersen, R. Wester, O. Heber, A. Lafosse, M. L. Rappaport, N. Alstein, and D. Zajfman, Phys. Rev. A **61**, 060705(R) (2000).
[20] N. Dudovich, B. Dayan, S. M. Gallagher Faeder, and Y. Silberberg, Phys. Rev. Lett. **86**, 47 (2001).
[21] W. J. Van Der Zande, W. Koot, and D. P. De Bruijn, Chem. Phys. **115**, 297 (1987).
[22] R. J. Le Roy and G. T. Kraemer, *BCONT 2.2. Computer Program for Calculating Absorption Coefficients, Emission Intensities or (Golden Rule) Predissociation Rates*, University of Waterloo Chemical Physics Research Report CP-650R^2 (2004).